

Winter climate anomalies in Europe and their associated circulation at 500 hPa

Klaus Fraedrich¹, Christian Bantzer², Ulrike Burkhardt³

¹ Meteorologisches Institut, Universität Hamburg, W-2000 Hamburg 13, Germany

² Department of Atmospheric Sciences, University of Washington, Seattle, USA

³ Meteorologisches Institut, Universität München, München, Germany

Received May 1, 1992/Accepted July 14, 1992

Abstract. Regional anomalies of the surface climate over Europe are defined by a simultaneous EOF-analysis of the normalized monthly mean sea level pressure, temperature and precipitation fields of 100 winters (December–February, 1887–1986) at 40 stations. The monthly amplitudes of the first EOF (about 25% of the total variance) are used as an index for the monthly winter climate anomaly. They characterize a high (low) pressure cell over central Europe associated with a positive (negative) temperature and precipitation anomaly over northern (central-southern) Europe as indicated by a northward (southward) shift of the tail end of the cross-Atlantic cyclone track. These patterns resemble the phenomenological anticyclonic (cyclonic) Grosswetter classification and the European blocking (enhanced zonal flow) regime. The second EOF is of similar magnitude and gives latitudinal corrections to these two basic flow regimes. The joint probability distribution of both amplitudes shows a weak bimodality mainly associated with the first EOF. Further insight into the underlying physical processes of the climate anomaly patterns in Europe is obtained from the extended Eliassen-Palm flux diagnostics of the barotropic transient eddy-mean flow interaction (Hoskins et al. 1983) and the stationary wave propagation (Plumb 1985). The diagnostics confined to the barotropic components and applied to the regression and the composite anomaly fields of the transient and stationary eddy flows of the 500 hPa geopotential (1946–87, north of 20°N) leads to the following results: (1) The bandpass filtered transient eddy variances of the 500 hPa geopotential show a shift of the cross-Atlantic storm track: In high (low) pressure situations over Europe the cross-Atlantic storm track intensity is enhanced (reduced) and its tail end is shifted northward (remains zonal); the North Pacific storm track extends further (less) eastward and thus closer to the west coast of North America. (2) The extreme high pressure system over Europe tends to be supported by an anomalous transient eddy forcing of the mean flow stream-

function: it enhances the zonal wind to its north and generates anticyclonic vorticity about 10° upstream from its center. In the low pressure composite the anomalous cyclonic vorticity is generated reducing the zonal flow to its north. (3) The occurrence (lack) of a strong eastward stationary wave activity flux over the Atlantic is associated with the high (low) pressure situations over Europe. Finally, a positive feedback is conjectured between the stationary wavetrain modifying the tail end of the cross-Atlantic storm track and the transient eddies intensifying this anomaly.

Introduction

The extended Eliassen-Palm flux vector (defined by Hoskins et al. 1983) is a prominent diagnostic tool amongst those developed for analyzing eddies and eddy-mean flow interaction in a zonally asymmetric atmosphere (see review in Holopainen 1984). The method is used to demonstrate the local interaction between transient eddies and the time mean flow. Many investigators have applied this eddy-mean flow diagnostic to study transient disturbances of the time mean flow using the observed and model atmospheres. There are, for example, case and composite studies of particular episodes like blocking (Trenberth 1986), various Atlantic-Europe weather regimes (Robertson and Metz 1990), patterns of teleconnection and storm track modes in the North Pacific and North Atlantic (Lau 1988), to name a few. Furthermore, there are model response studies on the forcing from sources in tropical (Held et al. 1989) and polar latitudes (Glowienka-Hense and Hense 1992) also applying this diagnostics.

In addition to the transient eddy-mean flow analysis, a stationary wave propagation diagnostic has been developed (Plumb 1985) as a further kind of eddy-mean flow analysis technique to explore the stationary perturbations of the zonal mean. So far, only few applications are available. Karoly et al. (1989) demonstrate the appli-

Formerly: Institut für Meteorologie, Freie Universität Berlin, W-1000 Berlin 41, Germany

Correspondence to: K Fraedrich

cability exploring horizontal quasi-stationary wave propagation in the Northern and Southern Hemisphere associated with prominent teleconnection patterns (ENSO, PNA). Somewhat related is a stationary wave response study (Ting and Held 1990; see also Held et al. 1989) in an idealized GCM, where both transient and stationary wave activity diagnostics have been applied to explore a feedback (and not simply the eddy-mean interaction) between both transient and stationary perturbations which helps to explain some of the puzzling results in ENSO response studies. In this sense we have used these two techniques and applied them simultaneously to climate anomalies in Europe to find out whether there are some indications of a transient-stationary eddy cooperation to transport signals over long distances (say, from a source which affects the sensitive tail end of the cross-Pacific storm track to a climate anomaly in Europe modifying the tail end of the cross-Atlantic storm track). The motivation for this study was initiated by phenomenological observations on El Niño warm and cold events and their possible association with the Grosse-wetter in the eastern North Atlantic/European sector, the weather patterns of some anomalous winter months in Europe and the positions or frequencies of the cross-Atlantic cyclones (van Loon and Rogers 1981; Kiladis and Diaz 1989; Fraedrich 1990). Of course, most of these results describe the ENSO response merely ‘after the fact’, which, however, is implicit in many of these response studies which are sensitive to small changes of the initial and boundary conditions.

In this study we apply the transient and stationary eddy diagnostic to circulation patterns associated with climate anomalies of winter months in Europe which may be interpreted as a response to unknown sources of transient and stationary wave activity fluxes. The aim is twofold: firstly, to identify a climate anomaly in Europe based on hundred year time series at 40 stations (second Section); secondly, to describe the interaction between the transient eddies and the anomaly states (third Section) and to locate possible source regions of the associated stationary wave propagation (fourth Section). As the latter may be one of the possible origins for an anomalous response in Europe, we speculate, in the discussion, about a possible feedback mechanism, which needs to be subjected to further tests.

Climate anomaly patterns in Europe: pressure, temperature and precipitation

Data

European climate anomaly patterns of the winter months (December, January and February) are constructed by simultaneous EOF (empirical orthogonal function) analysis. The data set consists of hundred years (1887–1986) of monthly mean sea level pressure, temperature, and precipitation at 40 stations (Table 1) which are selected to give an optimally homogeneous distribution over Europe. Unreduced surface pressure values at some stations were reduced to sea level values

Table 1. European stations with observations of sea level pressure (p), temperature (T) and precipitation (RR) used in this study

Station	T	p	RR	Station	T	p	RR
Aberdeen	×	×	×	Lisbon	×	×	×
Archangel		×	×	Madeira	×	×	×
Astrakhan	×			Madrid	×	×	×
Athen		×		Milan			×
Bergen	×	×		Mallorca	×	×	
Berlin	×	×	×	Marseilles	×	×	×
Bodø	×	×	×	Moscow	×	×	×
Breslau	×	×	×	Nantes	×	×	×
Budapest	×	×	×	Odessa	×	×	
Bucharest	×	×	×	Oktyabrski			×
De Bildt		×	×	Oslo	×	×	
Frankfurt/Main	×	×		Östersund			×
Geneva	×	×	×	Paris	×	×	×
Gothaab		×		Rome			×
Haparanda	×	×	×	Sibiu	×		×
Helsinki	×	×	×	St. Petersburg	×	×	×
Karesuando			×	Stykkisholmur	×	×	×
Kazan	×	×	×	Sulina	×	×	
Kiev	×	×	×	Valentia	×	×	×
Copenhagen	×	×	×	Vienna	×	×	×

Table 2. The contribution of the ranked climate state eigenvectors to the total variance: simultaneous pressure, temperature and precipitation field (p, T, RR); and pressure only (p only)

EOF:	1	2	3	4	5	6
p, T, RR:	24.8	22.7	9.4	5.4	4.9	2.6
p only:	44.2	26.9	11.1	4.7	3.9	2.4

using the observed monthly mean temperature. The data are taken from the World Weather Record (to 1970) and Berliner Wetterkarte (from 1971). Occasionally missing observations are replaced by its corresponding monthly climate mean. Note that not all variables are available at each station.

Data analysis

These three climate variables are comprised into a single standardized climate state vector whose components are defined as normalized anomalies of the sea level pressure, p , the temperature, T , and the precipitation, RR . This leads to a 95-dimensional European climate state vector comprising $\mathbf{p}(t)$, $\mathbf{T}(t)$, $\mathbf{RR}(t)$ at all stations:

$$\mathbf{X}(t) = \{\mathbf{p}(t) \mathbf{T}(t), \mathbf{RR}(t)\}$$

That is, each vector component, $x(t) = \{x(t) - \langle x \rangle\} / \langle \{x(t) - \langle x \rangle\}^2 \rangle^{1/2}$, is given by an anomaly or deviation from the ensemble mean of each month, $\langle \rangle$, normalized by its standard deviation. The subsequent empirical orthogonal function (EOF) analysis is applied to all winter months (December, January, February) to obtain a set of 95 eigenvectors. They are ranked by their contribution to the total variance (given by their eigenvalues, Table 2). These ‘Europe eigenvectors’ (see Kutz-

bach 1967 for a study of North American eigenvectors) represent states of European climate anomalies containing information on the simultaneous distribution of the sea level pressure, temperature and precipitation. They are used to reconstruct the original anomaly state vector by their respective principal components (PCs or amplitudes $E1(t)$, $E2(t)$ etc.):

$$\mathbf{X}(t) = E1(t) \cdot \text{EOF1} + E2(t) \cdot \text{EOF2} + \dots$$

The first two eigenvectors, EOF1 and EOF2 describe almost the same amount (about 25% each) of the total variance, whereas the third drops below ten percent. A hypothetical degeneracy of these two EOFs, whose eigenvalues should differ by the estimated standard deviation of either (see North et al. 1982) is excluded as follows:

1. Rotation of the simultaneous EOFs shows similar patterns retaining the basic structures of the unrotated. It is commonly assumed that this indicates that the patterns are representative in themselves (see, for example Mo and Ghil 1987).

2. The eigenvalues of the first and second EOF calculated from the pressure field alone (Table 2) are significantly different to one another according to the rule of thumb (North et al. 1982) and thus are the patterns. These two EOFs show structures which are very similar to the pressure fields of the simultaneous EOF analysis of pressure, temperature and precipitation. In addition, the correlation between the amplitudes of the first EOFs (that is, the single pressure and the simultaneous fields) is 0.9, which explains about 80% of each others variance. Furthermore, the first two EOFs of the temperature fields alone are similar to those of the simultaneous analysis but with inverse ranking (the relative contributions to the total variance being 42.3% and 18.4%, respectively).

The spatial structures (EOFs, Fig. 1)

The geographical patterns of the first and second EOF are presented in Fig. 1 and briefly discussed as follows:

1. The first EOF1 shows a marked pressure anomaly over continental Europe extending from Ireland to the Black Sea. In high pressure situations with enhanced anticyclonic ‘grosswetter’ the European continent is expected to be associated with a northward shift of the tail end of the cross-Atlantic storm track. Thus positive (negative) temperature and precipitation anomalies associated with the passage of frontal systems occur in the northwestern (southeastern) part of Europe. In low pressure situations, a negative pressure anomaly extends over the European continent. The related more southward position of the cyclone track and its associated frontal systems leads to enhanced precipitation and positive temperature anomalies in the central and southern parts of Europe.

2. The second EOF2 shows a marked north-south pressure gradient over Europe related to an enhanced (reduced) zonal flow which is associated with temperature and precipitation fields of positive (negative) anomalies

over central and northern Europe. These EOF2 fields basically show a correction to the EOF1 structure which leads to a modification of its north-south position.

Here it should be pointed out that the EOFs are dependent on the domain analyzed. However, independent analyses of weather regimes in the Atlantic/European sector lead to qualitatively similar results of which two examples may suffice: the 29 European Grosswetter types or large scale circulation regimes are conveniently combined to the prominent alternating cyclonic-anticyclonic circulation states (Hess and Brezowsky 1977) for further statistical analyses on circulation anomalies; the blocking pattern over Europe and the enhanced zonal flow are the two most frequently observed weather regimes in the North Atlantic/European sector (Vautard 1990).

The time structures (E1 and E2)

The amplitudes of the first and second EOF, $E1(t)$ and $E2(t)$ (principal components, PCs) are obtained for all 300 months after projecting the vector time series, $\mathbf{X}(t)$, onto the eigenvectors. The values of the two PCs are presented in Table 3 as a joint distribution. The following results are noted:

1. The first EOF amplitude, $E1$, indicates bimodality in the marginal distribution which appears to be more obvious in the joint distribution of the two PCs. The second PC, $E2$, is almost Gaussian and the bimodal centers lie only slightly off the $E2=0$ axis. Here it should be noted that the joint $E1$ and $E2$ distribution of the pressure field alone (not shown) also tends to bimodality which, however, is less obvious. It appears that the simultaneous treatment of the three climate variables enhances the signal of the climate state bimodality (as more physics is involved). Although not essential for the following study, a test of significance is of interest: The null-hypothesis that $E1$ is unimodally distributed, can be rejected on a 99% (88%) level of significance using a Monte Carlo test after Hansen and Sutera (1986, see Appendix) counting the percentage of bimodal samples produced by random numbers of normal (unimodal) distributions fitted to the data. Note however, that the null-hypothesis ($E1$ is Gaussian distributed) cannot be rejected using a Kolmogoroff-Smirnow test, even at relatively low levels of significance.

2. The observed weak bimodality of European climate states provides some additional support for the bimodal probability density distribution observed in the general circulation in the wave number 2 to 4 amplitudes of NMC analyses of 16 winter seasons (e.g., Hansen and Sutera 1986): ‘one mode corresponds to an amplified large-scale wave pattern; the other to a predominantly zonal flow’. It is not surprising that the regional climate anomalies show a weaker bimodal structure than the hemispheric data using the contributions of wave numbers 2 to 4.

EOF1

EOF2

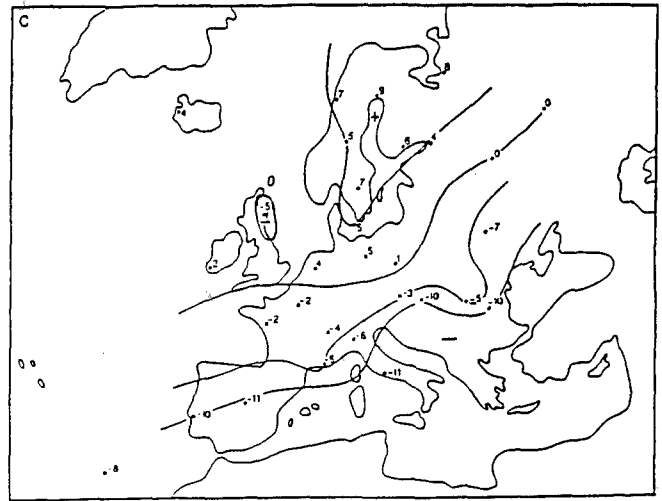
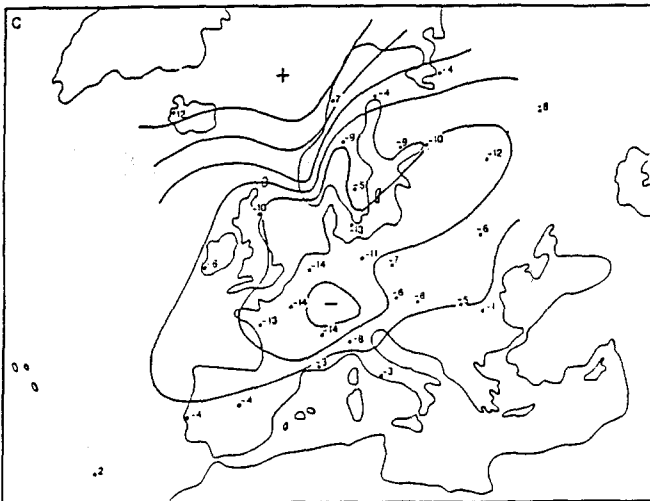
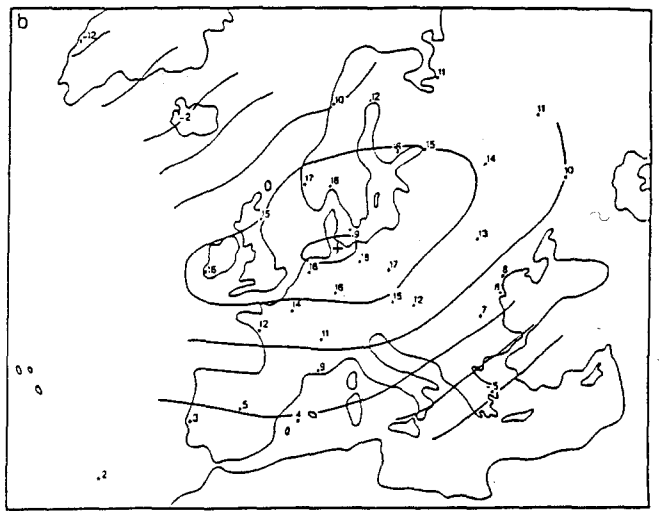
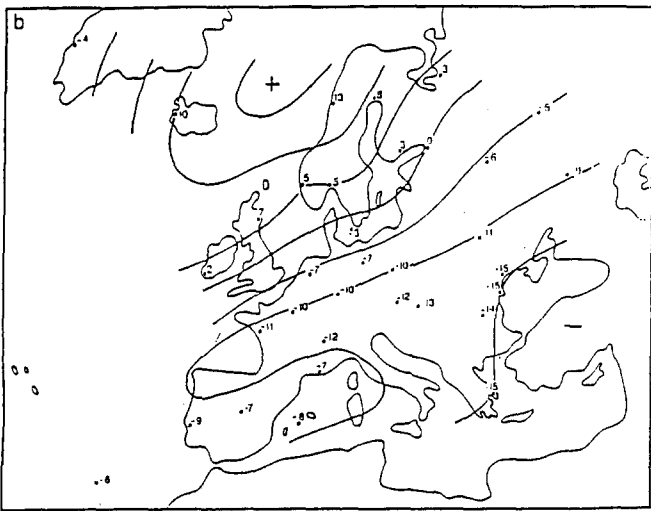
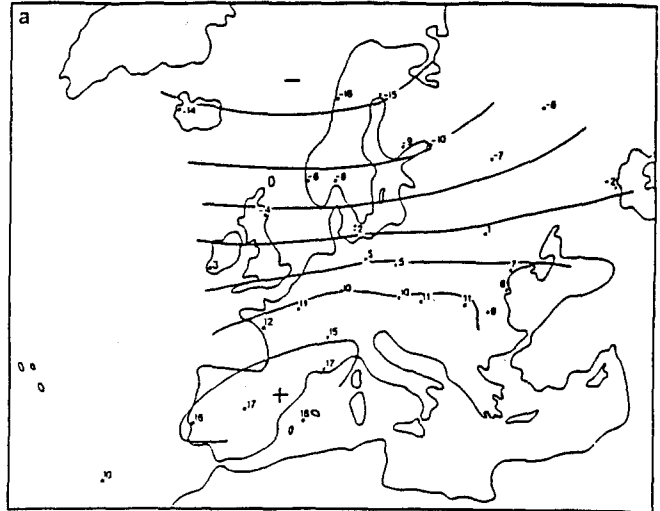
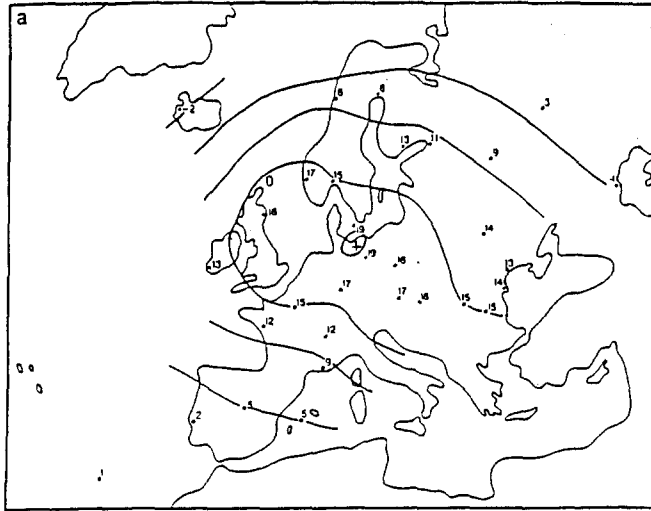


Fig. 1a–c. The geographical distribution of **a** monthly mean sea level pressure; **b** temperature and **c** precipitation over Europe based on hundred winter seasons (1887–1986): the first Europe ei-

genvektor of *EOF1* (this pattern corresponds to a positive principal component or E1-index) and the second Europe eigenvektor or *EOF2*

Table 3. The joint distribution of the monthly amplitudes E1 and E2 (principal components) of the first and second Europe eigenvector, EOF1 and EOF2

E1:	-30	-25	-20	-15	-10	-5	0	+5	+10	+15	+20	+25	+30
	0	2	8	17	26	52	45	41	45	40	17	6	1
E2:													
+30	0												
+25	1						1						
+20	9						1	5	1	2			
+15	28					4	4	3	8	4	3	1	1
+10	53			3	2	7	9	8	8	10	3	3	
+5	70	1	1	3	4	11	11	9	10	14	4	2	
0	51	1		3	7	13	4	7	6	7	3		
-5	51		6	4	4	13	9	3	8	1	3		
-10	22		1	3	5	3	1	5	2	1	1		
-15	9			1	2		4		2				
-20	5				2		1	1		1			
-25	1					1							
-30	0												
E2													

Table 4. The years (first two digits) and the number of the calendar month (last two digits) of the ten most extreme positive (negative) monthly amplitudes E1 of the first Europe eigenvector. This

index E1 defines high pressure or blocking (low pressure or zonal flow) anomalies in Europe with their associated temperature and precipitation fields

	1	2	3	4	5	6	7	8	9	10
E1 > 0:	59/2	64/1	53/12	63/12	72/12	56/2	71/12	75/2	49/2	48/12
E1 < 0:	48/1	65/12	77/2	66/2	81/12	57/2	84/1	55/2	70/2	79/12

A Europe climate anomaly index (E1)

All this suggests that the amplitude, E1 of the first EOF of the simultaneous climate state variable appears to be a useful index characterizing the climate anomaly state of winter months in Europe: the time series is highly correlated with the amplitudes of the significant first EOF of the pressure field alone which describes more than 40% of its variance. Therefore, further explorations of the dynamics associated with the two extremes of these climate anomalies in Europe will be based on this index (or PC). Note that the observed bimodality is not a necessary requirement but very helpful. For further reference and later composite analyses, the ten extreme months of positive and negative anomalies are documented in Table 4.

Transient eddy-mean flow forcing at 500 hPa

The data set and derived fields

The daily 500 hPa geopotential heights (NCAR, 5° × 5° grid, north of 20°N, 1946–1987, obtained from MPI für Meteorologie, Hamburg) comprise the 41 × 3 winter months analyzed in the following way. In this study, the analysis is based only on the geopotential height fields and the derived geostrophic wind. Both the original data set and a band-pass filtered dataset are used in this study; the latter is deduced applying the Blackmon and

Lau (1980) 21-point filter. It retains periods in the 2.5–6 day band and thus transient fluctuations of a time scale of less than a week. To obtain monthly averages of the band-pass filtered variances, the 10 days preceding and following the 90 day winter period were included for filtering. The following flow fields are subject to further analysis: (a) monthly mean geopotential heights, Z, and the derived mean geostrophic wind components, $\mathbf{V} = (U, V)$, are obtained from the daily data; (b) monthly variances $\langle z'^2 \rangle$, $\langle u'^2 \rangle$, $\langle v'^2 \rangle$ and the covariances of the geostrophic wind components, $[u'v']$, are deduced from the band-pass filtered dataset. The following ensemble averages are diagnosed:

1. The ensemble average of all 123 winter months describes the background climatology;
2. The temporal regression between NH circulation fields and the Europe climate index gives an estimate of the spatial extent and the intensity of the influence of the signal;
3. The ensemble averages (composites) of the ten extreme months with positive and negative indices of European climate anomalies (second Section) reveal asymmetries smoothed by regression.

The 500 hPa geopotential height and sea level pressure composites of the ten extreme winter months with positive/negative indices are presented in Fig. 2a–d. These ensemble averages show the upper ridge versus trough situation over Europe with the associated high and low pressure fields at sea level.

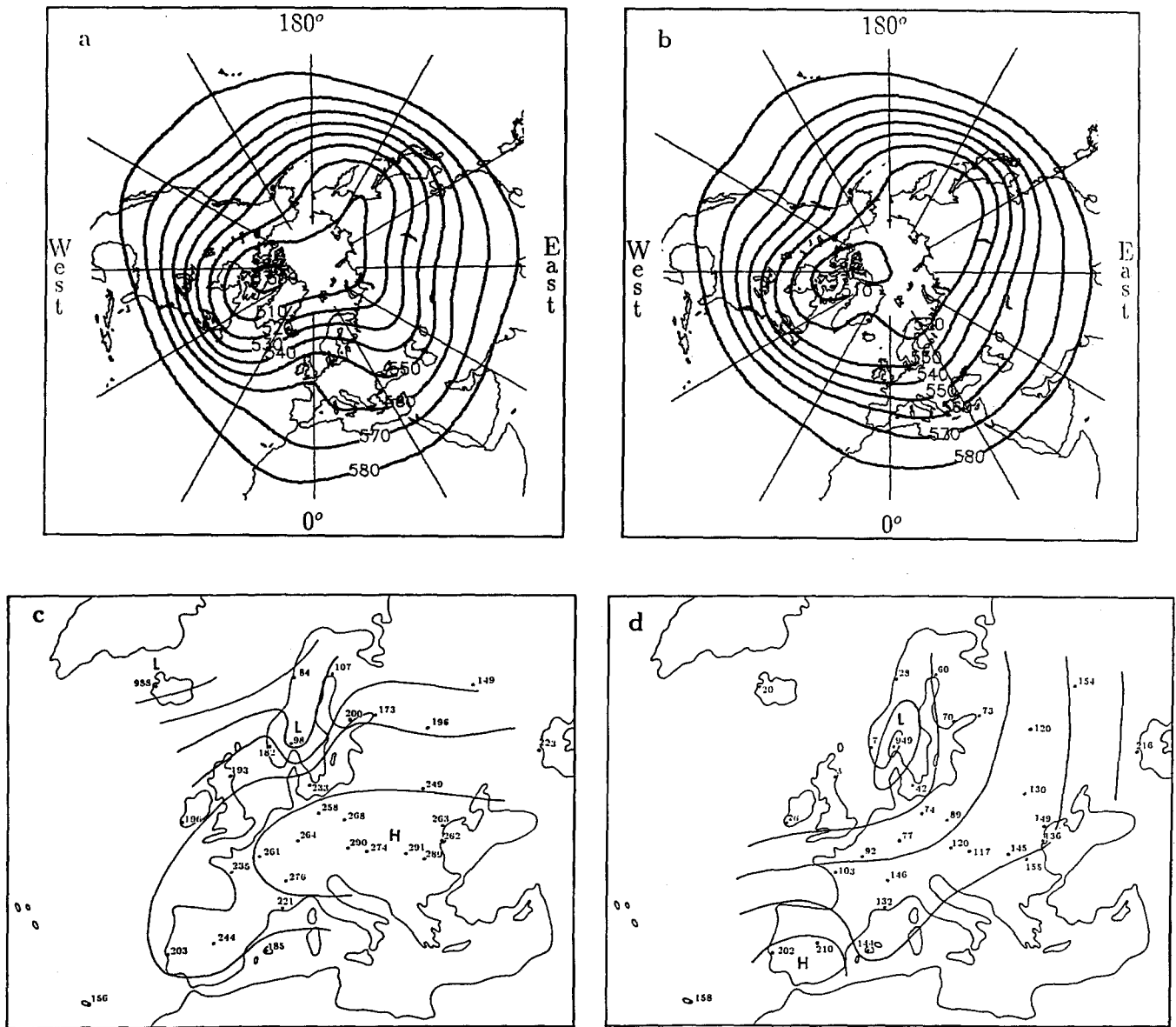


Fig. 2a-d. Composites of the ten extreme months with positive and negative indices of European climate anomalies in winter (Table 2): The 500 hPa height field for a positive and b negative indices and the sea level pressure field for c positive and d negative indices

Extended Eliassen-Palm vector

For zonal averaging, the Eliassen-Palm flux provides a diagnostic of both eddy behavior and its mean flow feedback. The extended Eliassen-Palm or **E**-vector has been introduced to constitute a diagnostic of the time averaged three-dimensional tropospheric flow which, in terms of the transient eddy vorticity flux, provides an interpretation of the eddy-mean flow interaction. Furthermore, the shape of the eddies and the sense of the group velocity can also be determined. The extended Eliassen-Palm or **E**-vector was introduced by Hoskins et al. (1983):

$$\mathbf{E} = - \{ \langle u'^2 \rangle - \langle v'^2 \rangle ; \langle u'v' \rangle \}. \tag{1}$$

Under the realistic assumption that the zonal scale of the transient eddies is much larger than the meridional scale, the **E**-vector can be related to the barotropic con-

version of energy from transient eddies to the time mean flow, C , the eddy forcing of the mean flow, F , and of the mean stream function, S (more details are found in the Appendices):

$$C = -\mathbf{E} \cdot \text{grad } U; \quad S = -\text{grad}^{-2}(\text{div} \langle \mathbf{v}' \zeta' \rangle); \tag{2}$$

$$F = -S_y = \text{grad}^{-2}(\text{div} \langle \mathbf{v}' \zeta' \rangle_y)$$

The last two terms are approximated by $S \sim -\text{grad}^{-2}(\text{div } \mathbf{E})_y$ and $F = -S_y \sim \text{div } \mathbf{E}$. These quantities will be discussed in the following analysis.

The Northern Hemisphere winter climatology

Before proceeding to the winter anomalies in Europe, the diagnostic of Northern Hemisphere (NH) winter mean, which is based on an ensemble average of all 123 winter months, will be briefly discussed to give a first

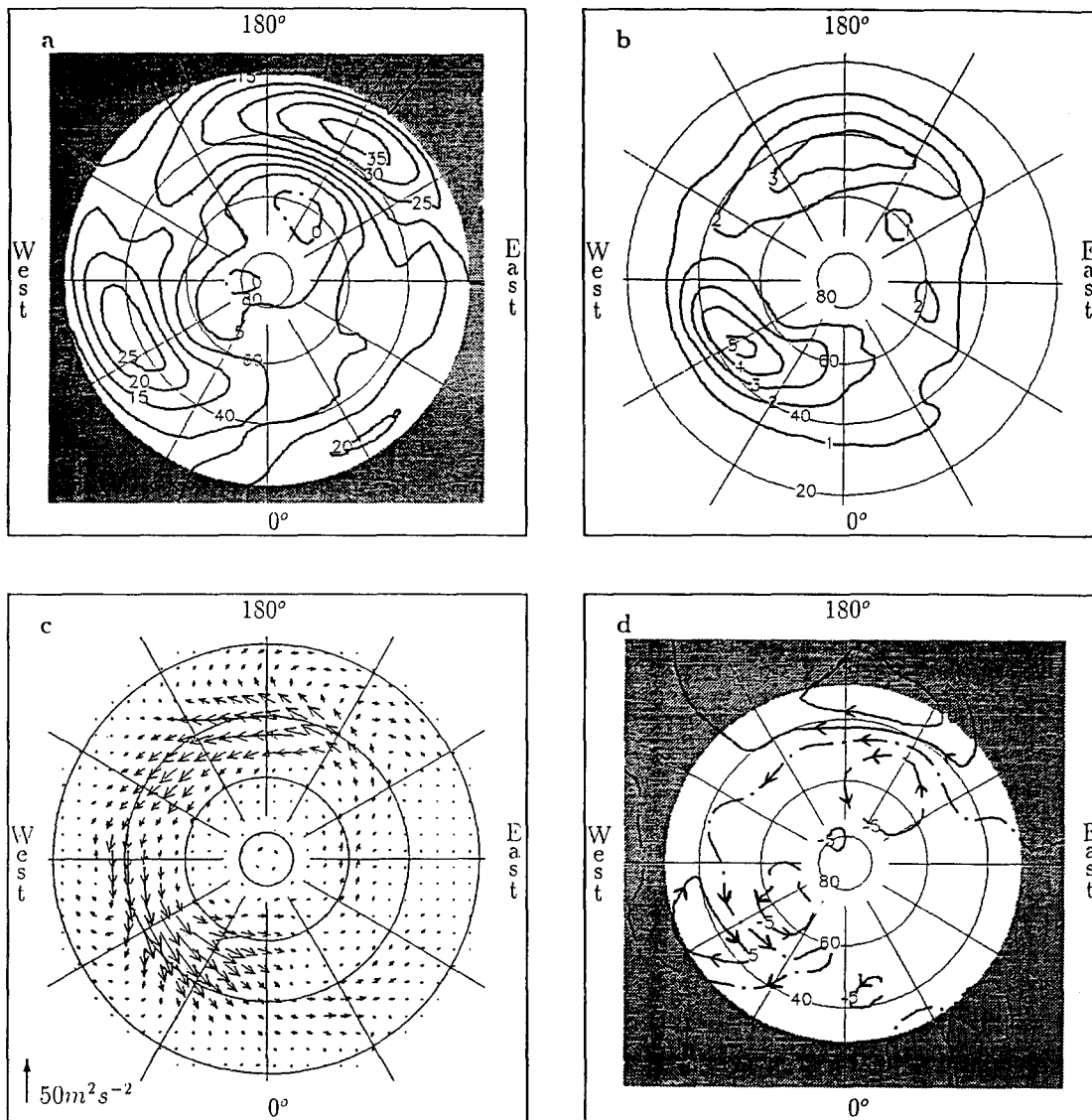


Fig. 3a-d. Climate mean state in winter: **a** 500 hPa geostrophic zonal wind (in m/s); **b** band-pass filtered geopotential height variance (contours in 10 gpdam²); **c** Eliassen-Palm flux (the arrow length in the lower left corresponds to 50 m²/s²); **d** source of the

mean stream function (contours in 5 m²/s²; a contour interval spread over 10° latitude corresponds to an acceleration of 0.4 m/s per day)

introduction to the methods applied (Fig. 3a-d). The familiar NH climatology of the mean geostrophic zonal wind field and transient eddy variance of the band-pass filtered geopotential heights reveals the following phenomenology of the subtropical jet and the storm tracks (see Wallace et al. 1988 on baroclinic wave guides, cyclone and anticyclone tracks). Strong zonal asymmetry is observed with jet exit regions over the oceanic sectors and the jet entrance over the continents; the associated variance maxima of the transient (band-pass filtered) geopotential heights lie towards the north of the jet exists over the oceanic sectors. Now, the results of the application of the **E**-vector diagnostic can be interpreted from different aspects which, however, are not independent:

Barotropic energy conversions. The **E**-vector is directed down the gradient of *U* in the jet exit (over most of the

oceanic sectors) indicating large energy conversions from the band-pass filtered transient eddies to the time mean flow; they transport westerly momentum westward toward the jet streams so that the time mean flow gains kinetic energy at their expense. Vice versa, in the jet entrance regions (over North America) the **E**-vector is directed up the gradient of *U* and the transient eddies gain kinetic energy at the expense of the mean flow. Furthermore, the band-pass filtered energy conversions over the North American/Atlantic sector are considerably stronger than over the North Pacific (see also Wallace and Lau 1985).

Forcing of the mean zonal wind *U*. The forcing of the time mean flow by the band-pass filtered transient eddies which, of course, is not independent of the barotropic energy conversion, can be deduced from the divergence of the **E**-vector field, $\text{div}\mathbf{E}$: “Where **E** is diver-

gent there is a forcing of the mean zonal circulation consistent with the tendency to increase the westerly mean flow" (and vice versa, Hoskins et al. 1983). As the spatial variations of the \mathbf{E} -vector along the storm tracks are generally weaker than in the traverse direction, the meridional components in $\text{div}\mathbf{E}$ dominate. At the centers of eddy activity, where $-\langle u'v' \rangle_y > 0$, eddy momentum transports tend to accelerate the westerly mean flow along the storm tracks which leads to a westerly acceleration north of the jet axis. Poleward (and farther south) of the zonally oriented storm track axis, where $-\{\langle u'^2 \rangle - \langle v'^2 \rangle\}_y > 0$ (and < 0), there are poleward (equatorward) accelerations affecting the meridional flow [assuming similarity with Trenberth's (1986) \mathbf{E} -vector diagnostic]. This is also observed by the fanning out of the \mathbf{E} -vectors at the eastern ends of the storm tracks (see Lau 1988).

Forcing of the mean stream function, $S = -\text{grad}^{-2} \{\text{div} \langle v' \zeta' \rangle\}$. This forcing is generally introduced to reduce the small-scale noise and to locate the sources and sinks of the mean stream function due to transient eddy activity (Fig. 3d). The most obvious feature is the anticyclonic forcing south of the storm tracks; it is associated with a westerly acceleration of the mean flow of about 1–2 m/s per day near the jet stream exits. Further results should be noted: in comparison with the single winter (1979/80) and 250 hPa analysis of Hoskins et al. (1983), our 500 hPa winter ensemble of 123 winter months shows (1) a stronger source region over the Pacific than over the Atlantic due to the fact that the 1979–80 season was unusual; and (2) a considerable westward shift in the position of the maxima which is due to the lower level analyzed. That is, the transient eddy activity propagates upwards originating from baroclinic instability at the lower levels and towards the east (shown in Hoskins et al. 1983).

Winter climate anomalies in Europe

In this subsection the flow regimes affecting the European winter climate anomalies and their associated anomalous circulation patterns are analyzed. The signal of the winter climate anomalies in Europe is discussed in terms of regression fields between the anomaly index and the circulation patterns. To demonstrate further details, composites (ensemble averages) of the ten most extreme cases are also used.

Jet stream/storm-track phenomenology (Fig. 4a–c)

The composites of the band-pass filtered monthly variances of the geopotential heights show a strong signal in the eastern North Atlantic-European sector. The sensitive tail end of the cross-Atlantic storm track is moved although the location of the origin in the western North Atlantic is relatively insensitive although its intensity changes. High (low) pressure anomalies over Europe are associated with enhanced (reduced) eddy activity in the

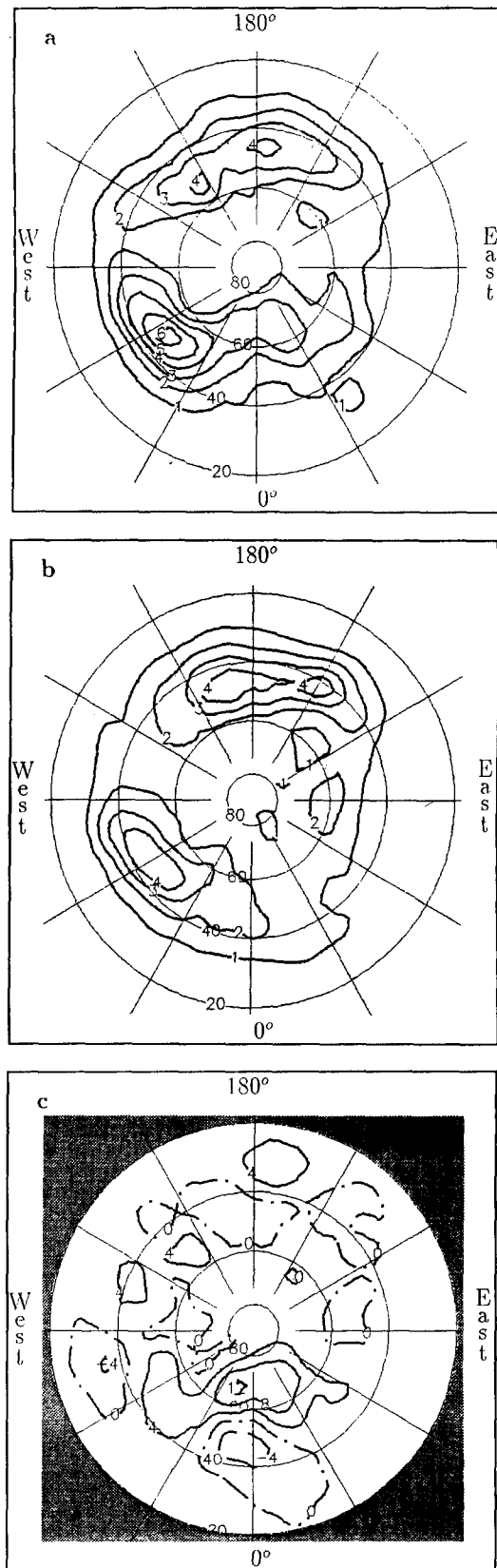


Fig. 4a–c. European winter anomalies: the composites of the band-pass filtered geopotential height variances $\langle z'^2 \rangle$ for a high and b low E1-index and c the regression field

region of cyclogenesis in the western North Atlantic, stronger (almost normal) jet maximum over the east coast of North America, and eddies following the northward (zonal) route of the tail end of the cross-Atlantic storm track. Furthermore, the composites reveal another interesting signal near the tail end of the cross-Pacific storm track. During high pressure situations (that is blocking or reduced zonal flow over Europe) the strongest activity of the transient eddies over the North Pacific extends about 10–20° longitude further eastward/southeastward and closer to the west coast of North America.

These results are implicit in the temporal regression between the transient eddy variance and the Europe anomaly index (E1). Positive regressions indicate that high (low) pressure anomalies over Europe are coincident with enhanced (reduced) transient eddy variance; the opposite holds for negative values. Thus, the dipole structure over the eastern Atlantic shows how the shift of the sensitive tail end of the storm track is associated with the climate anomalies in Europe. The correlations of above 0.4, which are associated with the regressions presented in Fig. 4c, in the storm track areas of the northeastern Atlantic, are clearly significant at the 95% level with 82 degrees of freedom (assuming two independent months per season). The correlation values of above 0.2 in the storm track area of the eastern Pacific just reach this 95%-level.

Eddy-mean flow diagnostic

The **E**-vector field of the high pressure composite ($E1 > 0$) shows relatively large intensities and an almost continuous stream of eastward directed **E**-vector bundles extending from the western North Pacific to the central North Atlantic (near 30° W). The northward bifurcation in the North Atlantic coincides with the observed storm track shift. The **E**-vectors in Fig. 5a show a strong convergence into the region near 55° N, 0° E, precisely where we see the easterly forcing of the mean flow in Fig. 5c. In northern Europe (where $\text{div}E > 0$) transient eddies generate westerly momentum through eddy-mean flow interaction supporting the mean anticyclonic vorticity and the high pressure anomaly over Europe (once initially established). In contrast, the low pressure anomaly composite is confined to a basically zonal **E**-vector flow in the North Atlantic basin without a northward shift or a prolongation of the storm track.

The regression of the NH streamfunction source, *S*, with the Europe anomaly (E1) index shows the following. Associated with positive (negative) anomalies one observes the source (sink) region at about 10° upstream (northwest) of the European anomaly in the area south of Iceland, where the storm track shift appears to have its largest effect on the zonal wind and vorticity anomalies. There is support from blocking studies (Mullen 1987; Lau 1988) which document similar relative positions of the streamfunction source.

Furthermore, there are negative regression coefficients over North America (along 50° N) describing en-

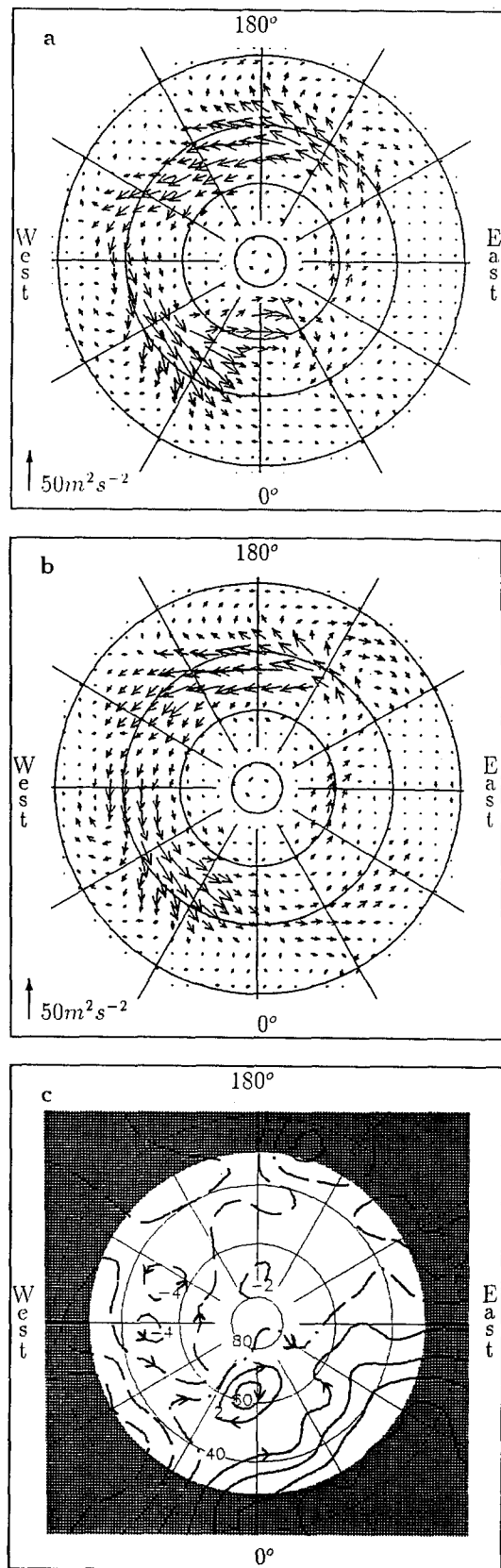


Fig. 5a-c. European winter anomalies: the associated *E*-vectors for a high and b low E1-index. Finally c the regression between the streamfunction source and the E1-index is also shown; the *arrows* are related to positive Europe anomaly indices and reverse orientation for negative ones

hanced cyclonic (anticyclonic) forcing due to transient disturbances related to a forcing of the mean flow in the jet entrance region. The divergence of the E-vector field (not shown), that is, the forcing of the zonal mean flow (Eq. 2), supports these findings.

Summary

Noting that the location but not the intensity of the cyclogenesis region, that is the origin of storm tracks, appears to be resilient to perturbations, whereas the sensitive tail end of a storm track is not, we observe the following. Associated with the extreme high pressure anomalies in Europe, the cross-Atlantic storm track is shifted towards a northern route. In this position the eddy-mean flow forcing leads to a westerly acceleration of the polar front jet thereby generating anticyclonic vorticity in the eastern Atlantic/European sector. Thus, an initially small positive anomaly over Europe appears to be necessary to generate a positive feedback through the subsequent storm track shift and the eddy-mean flow interaction enhancing the initially small anomaly. The missing link remains the generation of such an initially small high pressure anomaly over Europe. Furthermore, the tail end of the North Pacific storm track appears to extend farther to the east and closer to the American continent than in the low pressure composite. In addition, a mean flow forcing due to eddies in the jet entrance region over North America is observed.

The Europe low pressure composite realizes less eddy variance over the western North Atlantic with reduced intensity of cyclogenesis and the tail end of the cross-Atlantic storm track remains zonal entering, further downstream, into the European low pressure or zonal flow anomaly. Furthermore, a prolongation of the North Pacific storm track is not observed.

Stationary wave propagation in 500 hPa

Stationary wave propagation

A locally applicable conservation relation has been derived (Plumb 1985) for quasi-geostrophic waves on a zonal flow. The resulting relation provides a diagnostic of the three-dimensional propagation of stationary wave activity. This wave propagation diagnostic has been used in modeling studies of anomalous tropospheric stationary waves (Mo et al. 1987) and of stratospheric waves (Marks 1988). Most observational applications (see Karoly et al. 1989) are confined to the horizontal components, $\mathbf{F} = \{F_x; F_y\}$ of the three-dimensional stationary wave activity flux (following Eq. 4.9 of Plumb 1985; see also Appendix):

$$\mathbf{F} = \{F_x; F_y\} = \sigma/2f^2 \{Z_x^{*2} - Z^* Z_{xx}^*; Z_x^* Z_y^* - Z^* Z_{xy}^*\} \quad (3)$$

where $\sigma = p/1000$ hPa. The vector \mathbf{F} has been computed from the zonally asymmetric part of the time mean geopotential, Z^* , and mapped onto polar stereographic coordinates. The geopotential height fields, Z^*/g , and the wave activity flux are presented as in Karoly et al. (1989) and Plumb (1985).

Data

The following quantities derived from the daily 500 hPa geopotential heights (NCAR, $5^\circ \times 5^\circ$ grid, north of 20° N, 1946–1987 comprising 41×3 winter months) are subjected to stationary wave propagation diagnostics for further analysis: the monthly means of the geopotential height field, Z ; their zonal averages and the deviations from the zonal averages Z^* . As in the transient eddy-mean flow (third Section), the following ensemble averages enter the stationary wave propagation diagnostic: (1) the 123 winter months background climatology; (2) the regression between NH circulation fields and the Europe climate index; (3) composites of the ten extreme months with positive and negative index of European climate anomalies.

The Northern Hemisphere winter climatology

Before proceeding to the winter anomalies in Europe, the Northern Hemisphere (NH) winter climatology will be briefly discussed. The familiar NH climatological winter mean geopotential field reveals the dominant features of the deep troughs over the east coast of Asia and eastern North America with a succession of troughs and ridges covering most of the hemisphere (Fig. 6a). The wave activity flux (Eq. 3) is derived from the mean deviations, Z^* , of the zonally averaged height (Fig. 6b). It shows three major sources of the NH stationary wave activity: (1) the region of eastern Asia, (2) the western North Atlantic and (3) over the North Pacific/western North America. From eastern Asia the wave trains propagate predominantly eastward and equatorward with an indication of a zonal/equatorward bifurcation near 160° E. Emerging from the western North Atlantic/eastern North America, the wave trains propagate across the Atlantic and basically southeastward. Finally, in comparison with Plumb (1985), the source over western North America is not averaged out and wave trains, though weak, cross the North American continent. Except for the latter, the origins of the dominating wave trains are difficult to be directly related to an orographic source. An obvious alternative and substantial forcing mechanism (as suggested by Plumb 1985 and also evident from earlier El Nino-related wave train studies) is the diabatic heating, nonlinearity and/or a transient eddy momentum forcing. Over the western parts of the oceans this is accomplished in the zone of strong baroclinic development of the travelling disturbances; this occurs near the origin of the cross ocean storm tracks and, possibly to a lesser extent, along them. The apparent absence of significant propagation out of the tropics is not expected to be due to the poor observational coverage over tropical oceans. "It seems unlikely that a substantial wave train of large spatial scale could be missed altogether" (Plumb 1985) in the climatological average. This, however, does not imply their nonexistence in anomalous seasons.

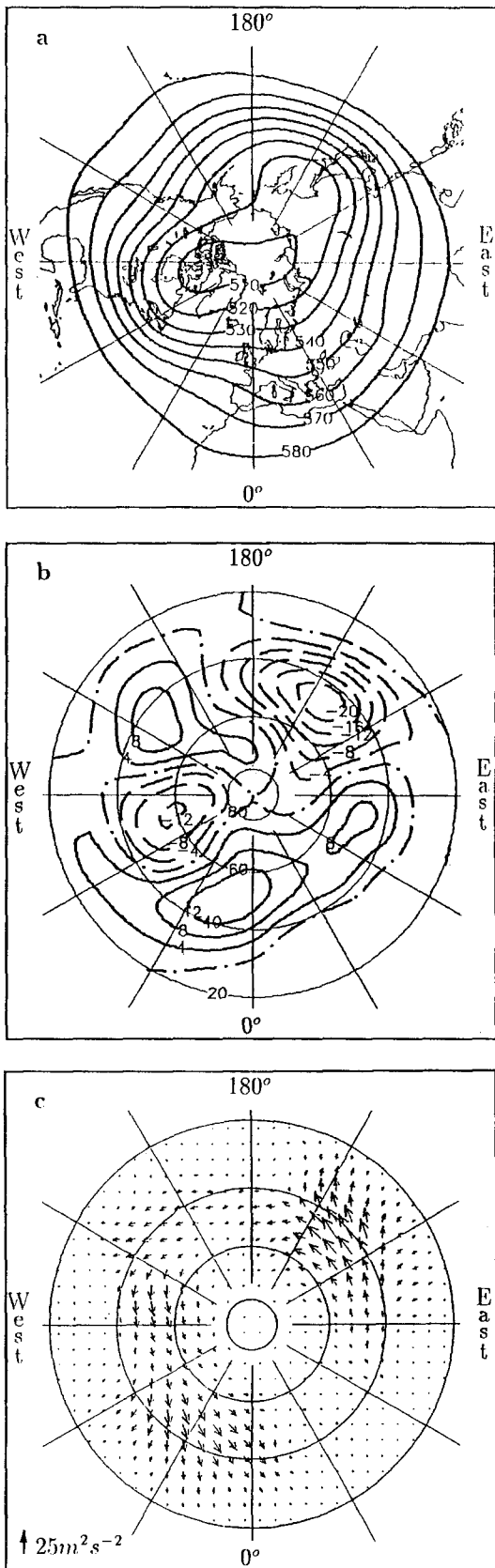


Fig. 6a-c. Climate mean state in winter: **a** 500 hPa geopotential height (in gpdam); **b** deviations from the zonal mean Z^* ; **c** stationary wave activity flux

Winter climate anomalies in Europe

The signal of the European winter climate anomalies and its association with stationary wave propagation is first analyzed in terms of regression fields (between the anomaly index, E1, and the height field). Additional details are demonstrated in the composites:

1. The regression of the European climate index, E1, with the 500 hPa heights reveals that the anomaly is not confined to the surface pressure fields over Europe but extends to higher levels. Further upstream and downstream one observes a sequence of alternating extrema (Fig. 7a, b). The horizontal wave activity flux vector shows an origin of the anomalous stationary wave propagation in the western North Atlantic from where wave trains emerge in the climate mean. It should be noted that the anomalous propagation vectors are more zonally oriented (Fig. 7b). Furthermore, the stationary wave fluxes associated with the Pacific transient eddy signal

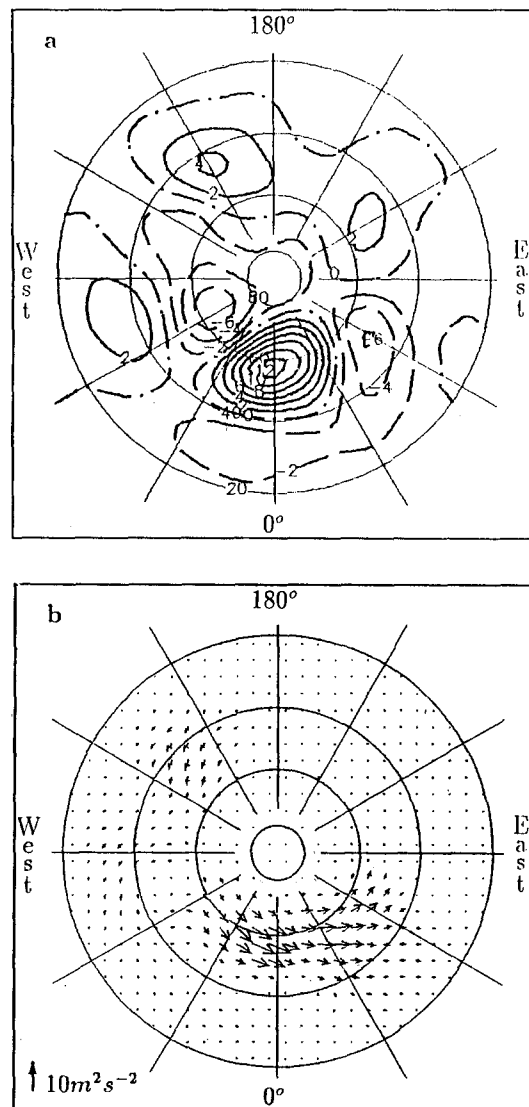


Fig. 7a, b. European winter anomalies: **a** stationary geopotential height fields for the E1-regression and **b** the associated wave propagation

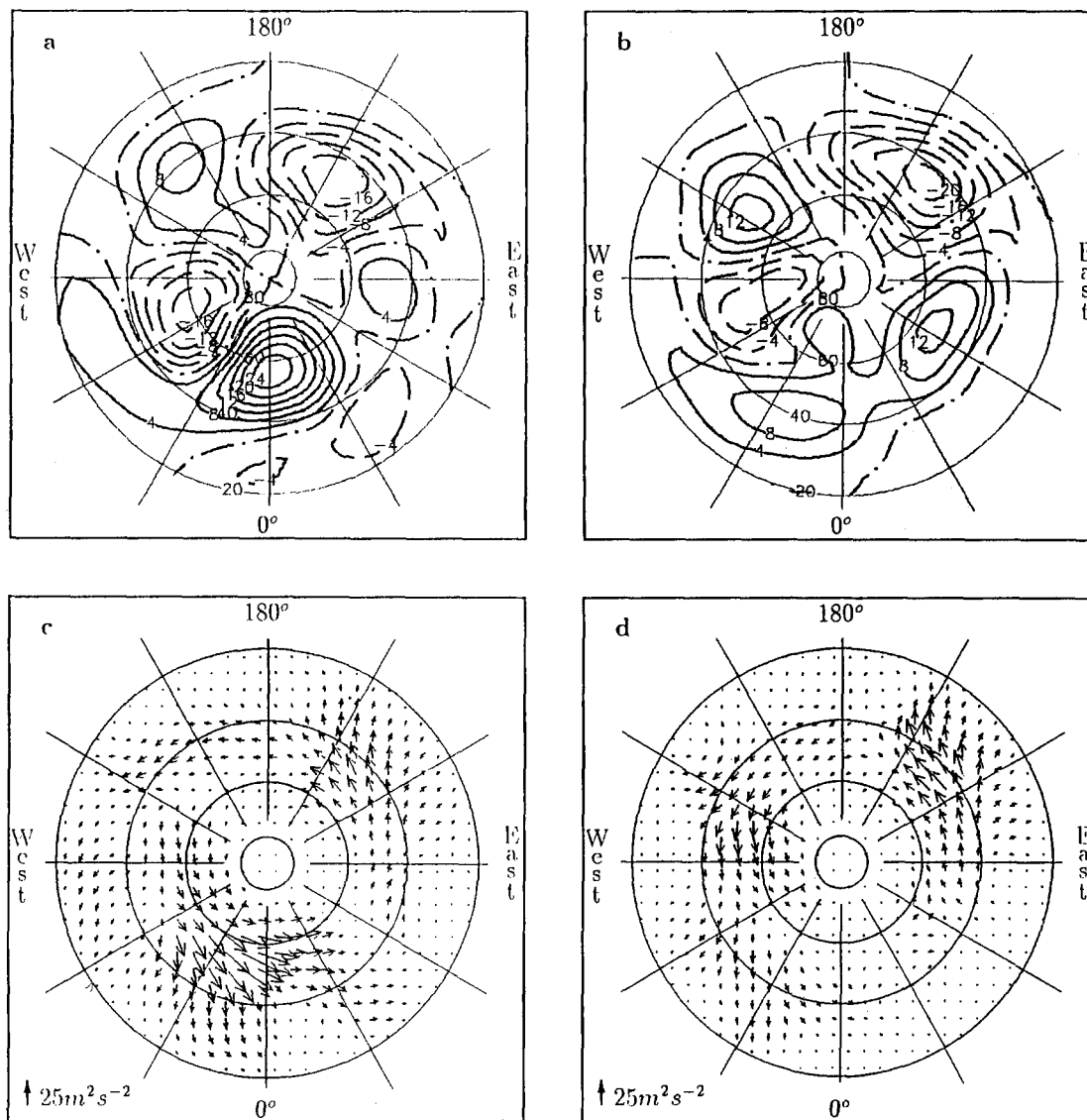


Fig. 8a–d. European winter anomalies: stationary geopotential height fields as deviations from the zonal mean, Z^* , for a positive and b negative composites; and c, d their associated wave propagation

(that is, the North Pacific storm track anomaly, Fig. 4a) are very weak.

2. The composite fields substantiate these results (Fig. 8): (a) The positive E1-composite shows a strong western North Atlantic source of stationary wave activity. The related wave activity flux vectors reveal a strong convergence over the eastern North Atlantic-European sector (Fig. 8a, c) supporting the high pressure anomaly over Europe. Wave propagation across North America is relatively weak compared with the negative E1-composite. (b) The reverse feature holds for the negative E1 composite (Fig. 8b, d); there is no substantial flux across the North Atlantic associated with a weaker positive deviation from the zonal mean. (Note that the regional climate mean over Europe has strong positive deviations from the zonal mean.) Stationary wave trains from the eastern North Pacific to the North American continent remain almost unchanged compared with the climate mean; they bifurcate into north-easterly and south-easterly routes (Fig. 8d).

Summary

Associated with the extreme high pressure anomalies in Europe, an intense stationary wave train emanates from the region of western Atlantic cyclogenesis, propagates across the North Atlantic and dissolves over the eastern Atlantic-European sector. This cross-Atlantic stationary wave flux does not exist in the European low pressure anomaly composite. Although observed simultaneously it may serve as the missing link generating an initially small, high pressure anomaly which shifts the sensitive tail end of the stormtrack northward.

Discussion

Simultaneous EOF-analysis of monthly mean sea level pressure, temperature and precipitation at 40 European stations for a hundred winter seasons (1887–1986) has revealed a bimodal structure of the surface climate ano-

maly state: a positive and negative anomaly of sea level pressure over continental Europe. These anomalies are associated with temperature and precipitation patterns which can be related to a shift of the sensitive tail end of the cross-Atlantic track of frontal systems. Although weak, this regional bimodal state resembles a bimodality documented for the NH general circulation wave number 2 to 4 amplitudes (Hansen and Sutera 1986) where “one mode corresponds to an amplified large scale wave pattern; the other to a predominantly zonal flow”. We feel that this justifies the circulation diagnostics to be applied to the European winter climate anomalies.

Both the transient and the stationary eddy mean flow diagnostics have been applied to 500 hPa geopotential height fields associated with the climate anomalies in Europe:

1. Positive anomalies in Europe (blocking or high pressure regimes) are related to a cross-Atlantic flux of stationary wave activity, whose source region is found at its western basin, coinciding with enhanced transient eddy variance. The location of the sink marks the high pressure anomaly over Europe and supports its state. The associated northward shift of the tail end of the cross-Atlantic transient eddy storm track generates westerly momentum of the mean flow in the north (or weakens the westerlies in the center) of the high pressure anomaly. That is, the high pressure anomaly is supported by anticyclonic vorticity generation. Moreover, there is an indication of transient eddy variance over the north-eastern Pacific extending further eastward with relatively intense E-vectors spreading from there across North America and into the North Atlantic basin.

2. Negative anomalies in Europe (that is, the low pressure or the zonal flow regimes) lack the cross-Atlantic stationary wave propagation whereas the situation over the North Pacific and North America is similar to the climatology. It appears that the North Pacific storm track (transient eddy variance) does not extend as far to the east.

Finally, for positive anomalies in Europe, we would like to propose a positive feedback mechanism between transient and quasi-stationary eddies in the North Atlantic basin, although the observed association between the signal in Europe and the eddy-diagnostics appears simultaneously in the monthly mean fields. Given a signal in the cyclogenesis area of the western Atlantic which acts as a source for stationary wave activity:

1. Then, a stationary wave train propagates across the Atlantic leading to an initially small anticyclonic or high pressure anomaly further downstream in the eastern Atlantic/European sector. This anomaly leads to a shift of the sensitive tail end of the cross-Atlantic storm track to a more northern route.

2. The subsequent eddy-mean flow interaction (that is the forcing of the mean flow by the transient eddies) induces anomalous westward accelerations, enhancing the polar front jet, north of this initially small high pressure anomaly and the anticyclonic vorticity in the anomaly region. That is, the initial high pressure anomaly generated by the stationary wave train is enhanced by the eddy-mean flow interaction.

There is some support in favor of this feedback speculation from results of idealized GCM experiments (Held et al. 1989; Ting and Held 1990). The ENSO signal over the North Pacific/American sector affects the tail end of the Pacific storm track which appears to be (initially) shifted by the Rossby wave train emanating from tropical sources. As this amplitude of the propagating stationary wave, however, has been shown (based on linear response studies) to be too small to account for the observed ENSO response, the transient eddy-mean flow mechanism is required: the induced shift of the sensitive tail end of the storm track amplifies the initial disturbance (a high pressure anomaly in the eastern North Pacific). However, this coupling between an initial stationary wave train and the subsequent enhancement of the mean flow by transient eddies may be (part of) the unique feature of a larger-scale weather regime in the North Atlantic/European sector (and not simply a positive feedback mechanism) because the signals occur almost simultaneously on a monthly time scale.

Although not substantiated by regression/correlation fields, the composites support the speculation that the positive North Atlantic-Europe anomaly might have its origin in the north-eastern Pacific and its storm track dynamics. Given a signal affecting the North Pacific storm track such that (1) the cross-Pacific storm track extends further to the east/southeast; then (2) more upper level Pacific depressions may have the chance to traverse North America (or enhance the jet entrance flow); (3) the remnants of these depressions (or the enhanced jet) intensify the baroclinic development in the cyclogenesis area of the western Atlantic (for example by non-normal mode instability, Farrell 1989); (4) this may provide the source required for stationary wave propagation across the Atlantic leading to the initial anticyclonic or high pressure anomaly downstream in the eastern Atlantic/European sector.

Furthermore, ENSO response studies in the eastern Atlantic/European sector indicate a far distant link between the Pacific and North Atlantic flow regimes (Kiladis and Diaz 1989; Fraedrich 1990): The “after the fact” ENSO effect on the European sector shows a pronounced frequency of cyclonic Grosswetter in Europe with weather patterns which resemble those represented by the low EOF1 index anomalies in Europe. These anomalies are associated with a reduced cross-Atlantic transient eddy-activity, the related high pressure anomaly suppressing cyclogenesis in the western North-Atlantic, and an enhanced stationary wavetrain across North America. Finally, it is known that the tail ends of storm tracks respond sensitively to a small (initial) perturbation which then is locally enhanced by the anomalous eddy activity through eddy-mean flow interaction; the locations of storm track origin, however, are rather insensitive and only their intensities are affected. It is plausible that such sensitive mechanisms for long distance connections can be evaluated only ‘after the fact’ and only in a statistical sense.

Again, it should be stressed that these conjectures are highly speculative and other interpretations of the data are conceivable. This will be subject to further research.

Acknowledgement. Thanks are due to R. Kuglin and K. Müller for the EOF analysis and Drs. Glowienka-Hense and Hense for comments. Part of this work is supported by a BMFT grant 'Analyse, numerische Simulation und Vorhersage natürlicher und anthropogener Klimaänderungen'.

Appendix 1.

Extended Eliassen-Palm vector:

$$\mathbf{E} = -\{\langle u'^2 \rangle - \langle v'^2 \rangle, \langle u'v' \rangle\}$$

1. Barotropic energy conversion (Wallace and Lau 1985)

The barotropic energy conversion from the transients to the time mean flow, $C = \langle u'^2 \rangle U_x + \langle v'^2 \rangle V_y + \langle u'v' \rangle \{V_x + U_y\}$, can be approximated (assuming $V_x \ll U_y$) to obtain the following form:

$$C = \{\langle u'^2 \rangle - \langle v'^2 \rangle\} U_x + \langle u'v' \rangle U_y = -\mathbf{E} \cdot \text{grad } U.$$

2. The eddy velocity covariance matrix (stress tensor)

The local velocity covariance matrix can be divided into an isotropic and anisotropic (trace free) part:

$$\begin{pmatrix} \langle u'^2 \rangle & \langle u'v' \rangle \\ \langle u'v' \rangle & \langle v'^2 \rangle \end{pmatrix} = \begin{pmatrix} K & O \\ O & K \end{pmatrix} + \begin{pmatrix} M & N \\ N & -M \end{pmatrix}$$

where $2K = \langle u'^2 \rangle + \langle v'^2 \rangle$; $2M = \langle u'^2 \rangle - \langle v'^2 \rangle$; $N = \langle u'v' \rangle$. The principle axes of the covariance tensor are oriented at the angle $\{\arctan(N/M)\}/2$ relative to the x-axis. Assuming Gaussian distributed fluctuations, u' , v' , the associated principle axes of the eddy-ellipses describe the statistically averaged shape of the disturbances and are related to the \mathbf{E} -vector (see Wallace and Lau 1985):

$$\mathbf{E} = \{\langle v'^2 \rangle - \langle u'^2 \rangle; -\langle u'v' \rangle\} = -\{2M, N\}.$$

3. Barotropic vorticity equation (see Hoskins et al. 1983; see also Trenberth 1986, Metz and Lu 1990)

The time-mean quasi-geostrophic barotropic vorticity, ζ , in a non-divergent and frictionless flow:

$$\zeta_t + \mathbf{V} \cdot \nabla \zeta + \text{div} \langle \mathbf{v}' \zeta' \rangle = 0$$

is forced by the divergence of the transient eddy vorticity flux. In Cartesian coordinates, the eddy vorticity flux and its divergence can be interpreted by the components of the extended Eliassen-Palm vector, $\mathbf{E} = -\{\langle u'^2 \rangle - \langle v'^2 \rangle, \langle u'v' \rangle\} = -\{2M, N\}$:

$$\langle \mathbf{v}' \zeta' \rangle = \{-M_y + N_x, -M_x - N_y\}$$

$$\text{div} \langle \mathbf{v}' \zeta' \rangle = -2M_{xy} + N_{xx} - N_{yy}$$

where $2M = \langle u'^2 \rangle - \langle v'^2 \rangle$ and $N = \langle u'v' \rangle$. Of additional interest is the eddy forcing of the mean streamfunction, $\Psi = \text{grad}^{-2} \zeta$, and of the mean zonal flow, U :

$$S = -\nabla^{-2} \text{div} \langle \mathbf{v}' \zeta' \rangle \quad \text{and} \quad F = -S_y = \nabla^{-2} (\text{div} \langle \mathbf{v}' \zeta' \rangle)_y$$

where $(\text{div} \langle \mathbf{v}' \zeta' \rangle)_y = \text{grad}^2 (2M_x + N_y) - M_{xxx}$. Assuming the x-scale to be much larger than the y-scale, the

last term, M_{xxx} , may be neglected so that the mean flow forcing yields:

$$F = -S_y = \nabla^{-2} (\text{div} \langle \mathbf{v}' \zeta' \rangle)_y = \text{div } \mathbf{E}.$$

4. Group velocity

In the barotropic case, the group velocity of the transient perturbations relative to the time mean flow has twice the angle of the \mathbf{E} -vector to the x-axis (provided the mean absolute vorticity gradient is meridional).

5. Computation

The inverse Laplacian operation has been solved by decomposing the eddy forcing term into spherical harmonics and then executing the inverse Laplacian in the spectral domain. The eddy forcing has been extrapolated from known values at 20°N to zero at the equator (see Lau 1988).

Appendix 2.

Stationary wave activity flux (Plumb 1985)

The conservation relation for the barotropic wave-activity, $A = \sigma q^{*2}/2Q_y$, has the form:

$$A_t + \text{div } \mathbf{F} = C,$$

where q^* is the eddy potential vorticity, Q is the steady zonal flow vorticity, and C contains the sources and sinks due to non-conservative effects and nonlinearity. For stationary waves the flux of wave activity.

$$\mathbf{F} = \{F_x; F_y\} = \sigma/2f^2 \{Z_x^{*2} - Z^* Z_{xx}^*; Z_x^* Z_y^* - Z^* Z_{xy}^*\}.$$

In the WKB limit and with the statement, $Z^* = Af\sigma^{-1/2} \sin(kx + ly)$, the flux \mathbf{F} reduces to the phase independent form:

$$\mathbf{F} \sim A^2 \{k^2, kl\}.$$

Since the group velocity for stationary waves is $\mathbf{c}_g = 2Q_y/K^4 \{k^2, kl\}$ with $\mathbf{K} = \{k, l\}$, $\mathbf{F} = K^4 A^2 c_g/2Q_y$ is parallel to the local group velocity. As a diagnostic tool the wave activity flux \mathbf{F} provides the following information:

For stationary waves $\text{div } \mathbf{F}$ is directly related to the sources and sinks of wave activity in the conservation relation. Thus $\text{div } \mathbf{F}$ localizes the generation or dissipation of stationary waves due to orography, diabatic heating and nonlinearity effects.

For almost plane waves \mathbf{F} is parallel to the group velocity, \mathbf{c}_g , and thus the propagation of stationary waves.

Appendix 3.

Test of bimodality (Hansen and Sutera 1986)

Since bimodality of a marginal distribution implies bimodality of the joint we restrict the test to the distribution of PC1. The test proceeds as follows: two unimodal distributions are fitted to the data to provide theoretical distributions which serve as parent distributions for random number generators. Thus, random samples and

their densities are constructed to count bimodality occurring by chance.

One of the unimodal distributions is Gaussian with the same mean and variance as the data; the second unimodal (but non-Gaussian) distribution is fitted to the data by the MPL-technique as follows.

MPL-Technique

A smooth distribution density estimate is obtained by the method of maximum penalized likelihood (MPL). This technique combines a maximization of the likelihood function and of the penalizing smoothness function. Smoothness is selected by a free parameter, a , just avoiding an inflection point between the two modes of the probability density (here the value is $a=1.3 \cdot 10^6$). The MPL method defines the maximum of the score function:

$$L(w) = \pi_i w(x_i) \exp -a \int |w_{zz}|^2 dz,$$

where x_i are the sample elements and w is any density with $\int w dz = 1$. "The discrete approximation of this equation can be solved with the IMSL routine DESPL (former NDMPLE). The free parameters to be supplied are the smoothness parameter a and the number of mesh points at which the probability density should be evaluated" (Sutera 1986). We used 27 mesh points to achieve a stable convergence of the iterative evaluation algorithm.

Now, the Monte Carlo test of bimodality proceeds in two steps: first the random number generator produces a set of random samples from the Gaussian and the second unimodal distributions (using IMSL routines RNGCS and RNGCT). Next, the distributions are evaluated using the MPL-technique again to estimate the number of bimodally distributed samples. Here we select the smoothness parameter which was sufficient to exhibit bimodality in the original data set ($a=6 \cdot 10^5$). We choose 200 random numbers for each sample to coincide with the assumed number of independent observations (2 per season). From 100 Gaussian distributed samples only one showed bimodality at the tail of the distribution. The 100 samples of the second unimodal distribution revealed twelve bimodal ones (that is 88% significance).

References

- Blackmon ML, Lau N-C (1980) Regional characteristics of the northern hemisphere winter time circulation: a comparison of a GFDL general circulation model with observations. *J Atmos Sci* 37:497-514
- Farrell BF (1989) Optimal excitation of baroclinic waves. *J Atmos Sci* 46:1193-1206
- Fraedrich K (1990) European Großwetter during the warm and cold extremes of the El Niño/Southern Oscillation. *Int J Climatol* 10:21-31
- Glowienka-Hense R, Hense A (1992) The effect of an Arctic Polynya on the Northern Hemisphere mean circulation and eddy regime: a numerical experiment. *Clim Dyn* 7:155-163
- Hansen AR, Sutera A (1986) On the probability distribution of planetary scale atmospheric wave amplitude. *J Atmos Sci* 43:3250-3265
- Held IM, Lyons SW, Nigam S (1989) Transients and the extratropical response to El Niño. *J Atmos Sci* 46:163-174
- Hess P, Brezowsky H (1977) Katalog der Grosswetterlagen. Ber Dtsch Wetterdienst, Offenbach, FRG
- Holopainen E (1984) Statistical local effect of synoptic scale transient eddies on time mean flow in the northern extratropics in winter. *J Atmos Sci* 41:2505-2515
- Hoskins BJ, James IN, White GH (1983) The shape, propagation and mean-flow interaction of large-scale weather systems. *J Atmos Sci* 40:1595-1612
- Karoly DJ, Plumb RA, Ting M (1989) Examples of the horizontal propagation of quasi-stationary waves. *J Atmos Sci* 46:2802-2811
- Kiladis GN, Diaz HF (1989) Global climatic anomalies associated with extremes of the Southern Oscillation. *J Climate* 2:1069-1090
- Kutzbach JE (1967) Empirical eigenvectors of sea level pressure, surface temperature and precipitation complexes over North America. *J Appl Meteorol* 6:791-802
- Lau N-C (1988) Variability of the observed midlatitude storm tracks in relation to low-frequency changes in the circulation pattern. *J Atmos Sci* 45:2718-2743
- Marks CJ (1988) Linear wavetrains in models of the stratosphere. *Quart J Roy Met Soc* 114:297-323
- Metz W (1986) Transient cyclone-scale vorticity forcing of blocking highs. *J Atmos Sci* 43:1467-1483
- Metz W, Lu M-M (1990) Storm track eddies in the atmosphere and in an ECMWF T21 climate model. *Beitr Phys Atmosph* 63:25-40
- Mo KC, Pfaendner J, Kalnay E (1987) A GCM study of the maintenance of the June 1982 blocking in the Southern Hemisphere. *J Atmos Sci* 44:1123-1142
- Mo KC, Ghil M (1987) Statistics and dynamics of persistent anomalies. *J Atmos Sci* 44:877-901
- Mullen SL (1987) Transient eddy forcing of blocking flows. *J Atmos Sci* 44:3-22
- North GR, Bell TL, Cahalan RF, Moeng FM (1982) Sampling errors in the estimation of empirical orthogonal functions. *Mon Wea Rev* 110:699-706
- Plumb RA (1985) On the three-dimensional propagation of stationary waves. *J Atmos Sci* 42:217-229
- Robertson AW, Metz W (1990) Transient-eddy feedbacks derived from linear theory and observations. *J Atmos Sci* 47:2743-2764
- Sutera A (1986) Probability density distribution of large scale atmospheric flow. *Adv Geophys* 29:319-338
- Ting M, Held IM (1990) The stationary wave response to a tropical SST anomaly in an idealized GCM. *J Atmos Sci* 47:2546-2566
- Trenberth KE (1986) An assessment of the impact of transient eddies on the zonal flow during a blocking episode using focalized Eliassen-Palm flux diagnostics. *J Atmos Sci* 43:2070-2087
- Vautard R (1990) Multiple weather regimes over the North Atlantic: analysis of precursors and successors. *Mon Wea Rev* 118:2056-2081
- Van Loon H, Rogers JC (1981) The Southern Oscillation; Part 2: Associations with changes in the middle troposphere in the northern winter. *Mon Wea Rev* 109:1163-1168
- Wallace JM, Lim G-H, Blackmon ML (1988) On the relationship between cyclone tracks, anticyclone tracks and baroclinic wave-guides. *J Atmos Sci* 45:439-462
- Wallace JM, Lau N-C (1985) On the role of barotropic energy conversions in the general circulation. *Adv Geophys* 28A:33-74